

STRUCTURAL, MORPHOLOGICAL AND ELECTRICAL PROPERTIES OF $\text{Ce}_{0.9}\text{Gd}_{0.1}\text{O}_{1.95}$

M.G. Chourashiya, S.S. Potdar and L.D. Jadhav*

Department of Physics, Shivaji University, Vidyanagar, Kolhapur, 416 004, India.

E-mail: lata_phy@unishivaji.ac.in

ABSTRACT

Intermediate temperature Solid Oxide Fuel Cell (IT-SOFC) shows number of advantages over high temperature SOFCs (HT-SOFCs), which includes smaller thermal mismatch between its components, rapid startup with less energy consumption etc. In the present paper, we are presenting the synthesis of ceria based oxygen ion conductor as an electrolyte for the low temperature SOFC. The bulk $\text{Gd}_{0.1}\text{Ce}_{0.9}\text{O}_{1.95}$ materials have been prepared using ceramic route. Since sintering of this oxide is a crucial parameter, which affects the micro-structural and electrical properties, the green pellets were sintered at 1400, 1500 and 1600 °C. The synthesized samples were characterized for their structural, elemental, morphological and electrical properties using XRD, EDAX, SEM and dc conductivity, respectively. The density measurements were done for estimation of porosity before and after sintering. The results will be presented and discussed at length in paper.

Keywords: Ceramic route, GDC10, IT-SOFC, Sintering, Electrical Properties.

1. INTRODUCTION

In recent past, materials for intermediate temperature solid oxide fuel cells (IT-SOFCs) have been researched extensively in view of advantages offered by IT-SOFCs over high temperature (HT) SOFCs. A less thermal mismatch between the cell components in IT-SOFC could solve the durability and performance degradation problem, while the low operating temperature may allow the rapid startup with low energy consumption. Of the cell components, an electrolyte is the heart of the cell and should have high ionic conductivity at low temperature (< 800°C). The oxygen ion conducting (OIC) materials such as doped LaGaO_3 , doped $\text{La}_{10}\text{Si}(\text{Ge})_6\text{O}_{27}$, doped $\text{La}_2\text{Mo}_2\text{O}_9$ and doped ceria have been investigated as an electrolyte for IT-SOFC. According to Steele (2001), OICs such as doped $\text{La}_{10}\text{Si}(\text{Ge})_6\text{O}_{27}$ and $\text{La}_2\text{Mo}_2\text{O}_9$ are unlikely to displace well established ceria based ceramic electrolytes, while it has been difficult to fabricate pure single phase $\text{La}_{0.9}\text{Sr}_{0.1}\text{Ga}_{0.8}\text{Mg}_{0.2}\text{O}_3$ (doped LaGaO_3) ceramic electrolytes. Selected ceramic proton conductors, e.g. $\text{BaZr}_{0.9}\text{Y}_{0.1}\text{O}_{2.95}$ can also exhibit ionic conductivity values approaching those of doped ceria at 500°C. However, ceramic fuel cells incorporating these materials will not be able to electrochemically oxidize CO, and do not appear to offer any advantages over the oxygen ion conducting electrolytes in this temperature region.

The gadolinium-doped ceria, with better properties than the other OICs, is most promising electrolyte for IT-SOFCs to be operated below 650°C (Sahibzada et al. 2000; Steele 2000b, 2001; and Zha S. et al. 2001). In the present paper, we are reporting the results of 10% gadolinium doped ceria (GDC10) synthesized by ceramic route. Since, ceramic route, a simple and cost-effective method, is often adopted to prepare bulk electrolyte materials (Wang et al. 1998 and Zhang et al. 2003a). As the sintering of such oxides is a crucial parameter in ceramic route, the GDC10 green pellets sintered at 1400, 1500 and 1600°C were characterized for its micro-structural and electrical properties. The variations in structural, morphological and electrical properties of GDC10 samples as function of sintering temperature and its duration have been discussed in detail.

* Corresponding author.

2. EXPERIMENTAL

2.1 Sample preparation

Commercially available powders of CeO₂ (AR, 99.9% HIMEDIA; make) and Gd₂O₃ (AR grade, 99.9 % HIMEDIA; make) were used as starting material. The powders of CeO₂ and Gd₂O₃ were mixed in stoichiometric proportions to obtain the GDC10 (Ce_{0.9}Gd_{0.1}O_{1.95}) compositions. Then the mixture was homogenized using agate-mortar. The mixed powder was calcinated at 750°C for 2 hrs and reground with agate-mortar. The powder was hardened with hydraulic press machine at pressure about 10–12 tons/inch² in circular disk shaped pellets. The green pellets were sintered at 1400 and 1500°C for 8 hrs and at 1600°C for 4 h in air. The un-sintered sample was identified as GDC1000 samples while the samples sintered at 1400, 1500 and 1600°C as GDC1014, GDC1015 and GDC1016, respectively. The heating rate of 3 K/min and cooling rate of 1 K/min was maintained for all samples.

2.2 Sample characterizations

The phase composition of the sintered GDC10 pellets was confirmed using X-ray diffractometer (PW-3710) with Cu-K_α radiation. The resultant XRD spectra were used to determine the crystallite size (*d*) and lattice parameter (*a*) of the samples. Density measurements were carried out for sintered samples to estimate the effect of sintering on its relative density and were related with SEM images. The surface morphology and the atomic ratio of the samples were revealed using scanning electron microscope (SEM, JEOL-JSM-6360) with attached EDAX unit. High magnification SEM was used to determine the average grain size using Cottrell method. The EDS spectrum of the prepared sample was used to confirm the expected atomic ratio. The dc-electrical conductivity of the samples was studied by two-probe method. The resultant plot of ln(σT) vs 1000/T used to obtain the activation energy for conduction.

3. Results and Discussion

3.1 Structural and morphological characterization

Figure 1 shows XRD patterns of un-sintered and sintered samples, which were compared with the JCPDS file no. 750161. All the samples showed the presence of (111), (200), (220), (311), (222), (400), (331), (420) and (422) reflection peaks in the scanning range 20–90° of 2θ. This confirms the ‘fcc’ structure of GDC10 sample. The XRD pattern of GDC1016 shows, tiny impurity peak due to Ce₂O₃ at 26.73°. The lattice parameter ‘*a*’ was calculated using the relation,

$$a = d \cdot \sqrt{h^2 + k^2 + l^2} \quad (1)$$

where, ‘*a*’ is the lattice parameter, ‘*d*’ the inter planner distance and ‘*hkl*’ are the Miller indices of the plane. The lattice parameter, ‘*a*’, is 5.4170Å for GDC1014, which increased to 5.4172Å for GDC1015, and to 5.4250Å for GDC1016. A very small increase in ‘*a*’ is due to high sintering temperature. The crystallite size of the samples sintered at different temperature was calculated using the Scherrer’s equation. The crystallite size is also observed to increase with sintering temperature and it increases from 407nm (GDC1014) to 670nm (GDC1016). Similar increase in lattice parameter and crystallite size was reported by Morris et al. (2006).

The energy dispersive X-ray analysis (figure 2) of pellets showed the presence of about 90 at% of Ce and 9 to 13 at% of Gd, which is in a fairly good agreement to the nominal composition of Ce_{0.9}Gd_{0.1}O_{1.95}.

The SEM of GDC1014, GDC1015 and GDC1016 pellet shown in figure 3(a-c) are uniform and dense. As expected, the surface morphology is improved with sintering temperature. The grain size is observed to increase from 2µm at 1400°C to 5µm at 1500°C, and to 11µm at 1600°C. GDC1014 sample have small porosity, which greatly reduced in GDC1015 and GDC1016. Further, more compact grains were observed for GDC1015 and GDC1016. The grain packing observed in SEM images is reflected in the relative density, which was calculated using the relation,

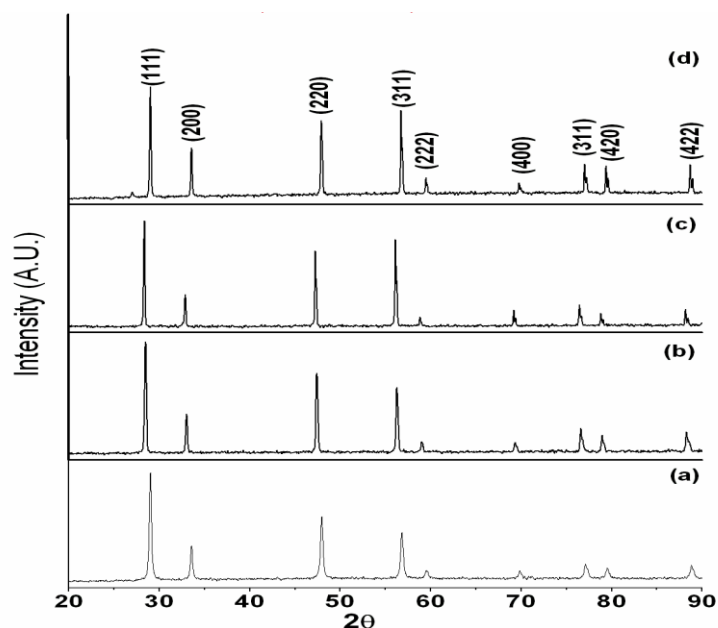


Figure 1. XRD patterns of (a) GDC1000, (b) GDC1014, (c) GDC1015 and (d) GDC1016.

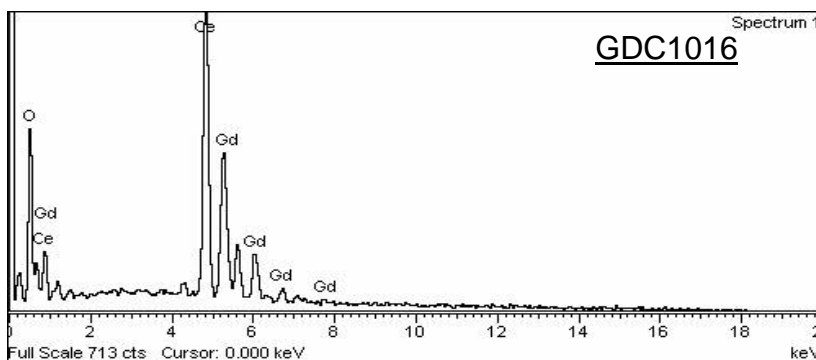


Figure 2. A typical EDAX of prepared sample (GDC1016).

$$\% \text{ density} = \frac{d_m}{d_{th}} \times 100 \quad (2)$$

where, d_m is the density of samples measured using Archimedes principle and d_{th} the theoretical density which is given by

$$d_{th} = \frac{4}{N_A a^3} \left[(1-x)M_{Ce} + x \cdot M_{Gd} + \left(2 - \frac{1}{2} \cdot x \right) M_O \right] \quad (3)$$

where, x is gadolinium content ($x = 0.1$), ' a ' the lattice constant at room temperature of GDC solid solutions, N_A the Avogadro number, and M refers to the atomic weight (Zhang et al. 2003b). The relative density for GDC1014 is 91% of theoretical value, which increased to 99% for samples sintered at 1500°C for 8h (GDC1015). For further increase in sintering temperature i.e. sintering at 1600°C for 4h (GDC1016), the relative density is lowered slightly to 98% of theoretical value. The decrease in the relative density is due to sintering carried out for shorter duration i.e. for 4h. Hence the sintering time in addition to sintering temperature plays the key role in morphological properties. The samples of our earlier work have shown the relative densities less than 90% of theoretical value (Jadhav et al. 2007).

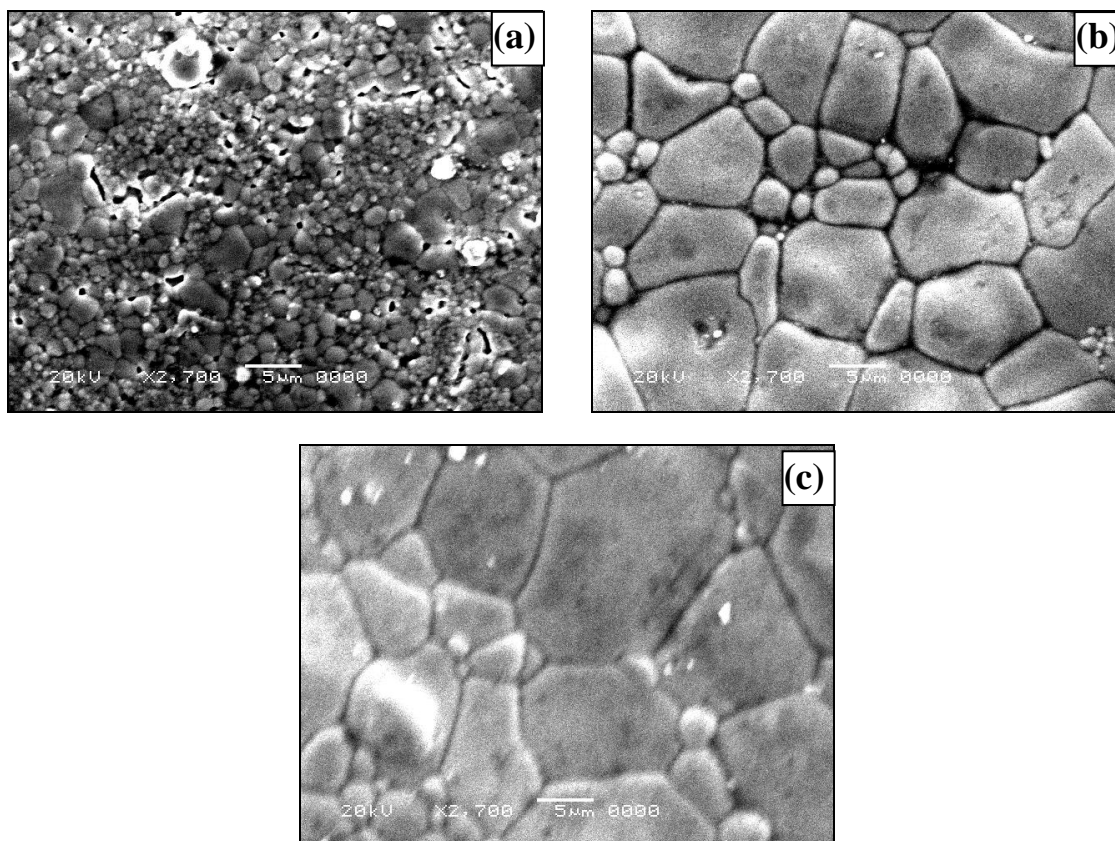


Figure 3. SEM of un-etched (a) GDC1014, (b) GDC1015 and (c) GDC1016.

3.2 Electrical conductivity measurement

The dc conductivity measurement was done by two-probe method in the temperature range 25 to 850°C. The variation of $\ln(\sigma T)$ with $1000/T$ for GDC10 pellets sintered at 1400°C, 1500°C and 1600°C is shown in figure 4. The plots showed the change in slope at around the 300°C and 650°C. The change in slope at 300°C is attributed to initiation of ionic diffusion and that at 650°C may be due to slight change in mechanism of conduction (Zha et al. 2003).

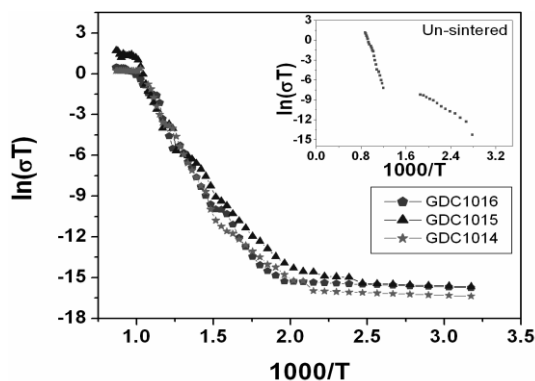


Figure 4. Variation of $\ln(\sigma T)$ vs $1000/T$.

The conductivity at 700°C is of the order of 10^{-3} S-cm⁻¹, which is lower than that of our earlier reported values (Jadhav et al. 2007). This is attributed to the fact that with increase in thickness of sample, ohmic losses increases

and hence decrease in conductivity (Steele B. C. H. 2000a). The thickness of pellets in earlier work was about 0.15–0.17cm, while in the present report it is 0.27–0.34cm.

Activation energies (E_a) for conductivity data were calculated by fitting the data to the Arrhenius relation for thermally activated conduction, which is given as,

$$\sigma = (\sigma_0 / T) \exp(E_a / KT) \quad (4)$$

where, E_a is the activation energy for conduction, T the absolute temperature, K the Boltzmann constant and σ_0 the pre-exponential factor. The activation energy is decreased from 2.24eV to 0.70eV (Table 1).

Table 1. Variation in activation energy of GDC10 samples with sintering temperature

| Sl. No. | Sample ID | Sintering Temperature (°C) | Activating energy (eV) |
|---------|-----------|----------------------------|------------------------|
| 1 | GDC1000 | Un-sintered | 2.24 |
| 2 | GDC1014 | 1400 | 1.04 |
| 3 | GDC1015 | 1500 | 0.80 |
| 4 | GDC1016 | 1600 | 0.70 |

4. CONCLUSIONS

The effect of sintering temperature on the structural, morphological and electrical properties of the GDC10 was investigated. The lattice parameter, a, was increased with sintering temperature. The surface morphology of the samples showed almost no porosity and grain size was increased with increasing sintering temperature. The maximum densification (99% of theoretical value) and conductivity was observed for the samples sintered at 1500°C for 8h and hence fulfill requirement of electrolyte for IT-SOFC.

ACKNOWLEDGEMENTS

The authors are very much thankful to DRDO for their financial support. Also the authors are thankful to UGC-DAE Consortium for Scientific Research, Indore for providing sintering and characterization facilities.

REFERENCES

- [1] Jadhav L.D., Pawar S.H., Chourashiya M.G., 2007, Effect of sintering temperature on structural and electrical properties of gadolinium doped ceria ($Ce_{0.9}Gd_{0.1}O_{1.95}$), *Bull. Mater. Sci.*, 30, 2, 97.
- [2] Morris V. N., Farrell R. A., Sexton A. M. and Morris M. A., 2006, Lattice constant dependence on particle size for ceria prepared from a citrate sol-gel, *J. Phy.-Conference Series: Imaging, Analysis and Fabrication on the Nanoscale*, 26, 119.
- [3] Sahibzada M., Steele B.C.H., Hellgardt K., Barth D., Effendi A., Mantzavinos D., Metcalfe I.S., 2000, Intermediate temperature solid oxide fuel cells operated with methanol fuels, *Chem. Eng. Sci.*, 55, 3077.
- [4] Steele B.C.H., 2000, Appraisal of $Ce_{1-y}Gd_yO_{2-y/2}$ electrolytes for IT-SOFC operation at 500C, *Solid State Ionics*, 129, 95.
- [5] Steele B.C.H., 2000, Materials for IT-SOFC stacks: 35 years R&D: the inevitability of gradualness, *Solid State Ionics*, 134, 3.
- [6] Steele B.C.H., 2001, Material science and engineering: the enabling technology for the commercialization of fuel cell systems, *J. Mater. Sci.*, 36, 1053.
- [7] Wang K., Ticky R.S., Goodenough J.B., 1998, Superior perovskite oxide-ion conductor; strontium- and magnesium-doped $LaGaO_3$: Phase relationships and electrical properties, *J. Am. Ceram. Soc.*, 81, 2565.
- [8] Zha S., Fu Q., Lang Y., Xia C., Meng G., 2001, Novel azeotropic distillation process for synthesizing nanoscale powders of yttria doped ceria electrolyte, *Mater. Lett.*, 47, 351.
- [9] Zha S., Xia C., Meng G., 2003, Effect of Gd (Sm) doping on properties of ceria electrolyte for solid oxide fuel cells, *J. Power Sources*, 115, 44.
- [10] Zhang T.S., Kong L.B., Zeng Z.Q., Huang H.T., Hing P., Xia Z.T., Kilner J.A., 2003, Sintering behavior and ionic conductivity of $Ce_{0.8}Gd_{0.2}O_{1.9}$ with a small amount of MnO_2 doping, *J. Solid State Electrochem.*, 7, 348.
- [11] Zhang T.S., Ma J., Huang H.T., Hing P., Xia Z.T., Chan S.H., Kilner J.A., 2003, Effects of dopant concentration and aging on the electrical properties of Y-doped ceria electrolytes, *Solid State Sciences*, 5, 1505.